

Theory of Pump-Probe Experiments of Metallic Metamaterials Coupled to a Gain Medium

Zhixiang Huang,^{1,2} Th. Koschny,¹ and C. M. Soukoulis^{1,3}

¹Ames Laboratory and Department of Physics and Astronomy, Iowa State University, Ames, Iowa 50011, USA

²Key Laboratory of Intelligent Computing and Signal Processing, Anhui University, Hefei 230039, China

³Institute of Electronic Structure and Laser, FORTH, 71110 Heraklion, Crete, Greece

(Received 17 October 2011; published 4 May 2012)

We establish a new approach for pump-probe simulations of metallic metamaterials coupled to the gain materials. It is of vital importance to understand the mechanism of the coupling of metamaterials with the gain medium. Using a four-level gain system, we have studied light amplification of arrays of metallic split-ring resonators with a gain layer underneath. We find that the differential transmittance $\Delta T/T$ can be negative for split-ring resonators on the top of the gain substrate, which is not expected, and $\Delta T/T$ is positive for the gain substrate alone. These simulations agree with pump-probe experiments and can help to design new experiments to compensate for the losses of metamaterials.

DOI: [10.1103/PhysRevLett.108.187402](https://doi.org/10.1103/PhysRevLett.108.187402)

PACS numbers: 78.67.Pt, 42.25.Bs, 78.20.Ci, 78.45.+h

The field of metamaterials has seen spectacular experimental progress in recent years [1–3]. Most metamaterials have a metal-based nanostructure and eventually suffer from conductor losses at optical frequencies, which are still orders of magnitude too large for realistic applications. In addition, metamaterial losses become an increasingly important issue when moving from multiple metal-based metamaterial layers to the bulk case [3]. Thus, the need for reducing or even compensating for the losses is a key challenge for metamaterial technologies. One promising way of overcoming the losses is based on introducing the gain material to the metamaterial. The idea of the combination of a metamaterial with an optical gain material has been investigated by several theoretical [4–7] and experimental studies [8–12]. From the experimental point of view, the realistic gain can be experimentally realized with fluorescent dyes [8], quantum dots [9,10], or semiconductor quantum wells [11,12]. All these loss compensations are mainly attributed to the coupling between metamaterial and the gain medium. Without sufficient coupling, no loss compensation can happen, nor can the transmitted signal be amplified. Therefore, it is of vital importance to understand the mechanism of the coupling between metamaterial and the gain medium. In addition, these ideas can be used in plasmonics to incorporate gain [13,14] to obtain new nanoplasmonic lasers [15,16].

In this Letter, we present a systematic theoretical model for pump-probe experiments of metallic metamaterials coupled with the gain material, described by a generic four-level atomic system. We describe the dynamical processes in metamaterials with gain; increasing the gain changes the metamaterial properties, and we need to have self-consistent calculations [4–6] to reach a steady state. The pump-probe results affect the time dependence of the population inversion and the electric field enhancement that increases the effective gain. We observe differential transmittance signals from the coupled system that

are larger than for the bare gain. Furthermore, we observe a more rapid temporal decay of the differential transmittance signal for the coupled system compared to the bare gain. Both effects indicate substantial local-field-enhancement effects, which increase the effective metamaterial gain beyond the bare gain, leading to a significant reduction of the metamaterial's losses.

We model the dispersive Lorentz active medium by using a generic four-level atomic system. The population density in each level is given by N_i ($i = 0, 1, 2, 3$). The time-dependent Maxwell's equations for isotropic media are given by $\nabla \times \mathbf{E}(r, t) = -\partial \mathbf{B}(r, t)/\partial t$ and $\nabla \times \mathbf{H}(r, t) = \partial \mathbf{D}(r, t)/\partial t$, where $\mathbf{B}(r, t) = \mu \mu_0 \mathbf{H}(r, t)$, $\mathbf{D}(r, t) = \epsilon \epsilon_0 \mathbf{E}(r, t) + \mathbf{P}(r, t)$, and $\mathbf{P}(r, t)$ is the dispersive electric polarization density that corresponds to the transitions between two atomic levels, N_1 and N_2 . The vector \mathbf{P} introduces gain in Maxwell's equations, and its time evolution can be shown to follow that of a homogeneously broadened Lorentzian oscillator driven by the coupling between the population inversion and external electric field [17]. Thus, \mathbf{P} obeys the equation of motion

$$\frac{\partial^2 \mathbf{P}(r, t)}{\partial t^2} + \Gamma_a \frac{\partial \mathbf{P}(r, t)}{\partial t} + \omega_a^2 \mathbf{P}(r, t) = \sigma_a \Delta N(r, t) \mathbf{E}(r, t),$$

where Γ_a stands for the linewidth of the atomic transitions at ω_a and accounts for both the nonradiative energy decay rate as well as dephasing processes that arise from incoherently driven polarizations. In the following simulations, this value is equal to $2\pi \times 20 \times 10^{12}$ rad/s. σ_a is the coupling strength of \mathbf{P} to the external electric field, and its value is taken to be 10^{-4} C²/kg. The factor $\Delta N(r, t) = N_1(r, t) - N_2(r, t)$ is the population inversion between level 2 and level 1 that drives the polarization \mathbf{P} . In order to do pump-probe experiments numerically, we first pump the gain material with a short, intense Gaussian pump pulse. After a suitable time delay, we probe the structure with a weak probe pulse (see Fig. 1). In our model, an

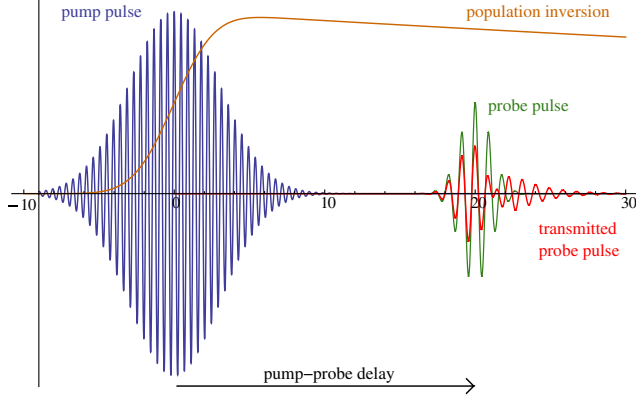


FIG. 1 (color online). Schematic illustration of pump-probe experiments.

external mechanism pumps electrons from the ground state level N_0 to the third level N_3 by using a Gaussian pumping $P_g(t)$, which is proportional to the pumping intensity in the experiments. After a short lifetime τ_{32} , electrons transfer nonradiatively into metastable second level N_2 . The second level (N_2) and the first level (N_1) are called the upper and lower lasing levels, respectively. Electrons can be transferred from the upper to the lower lasing level by spontaneous and stimulated emission. At last, electrons transfer quickly and nonradiatively from the first level (N_1) to the ground state level (N_0). The lifetimes and energies of the upper and lower lasing levels are τ_{21} , E_2 and τ_{10} , E_1 , respectively. The center frequency of the radiation is $\omega_a = (E_2 - E_1)/\hbar$, which is a controlled variable chosen according to the pump-probe experiments. The parameters τ_{32} , τ_{21} , and τ_{10} are chosen to be 0.05, 80, and 0.05 ps, respectively. The initial electron density $N_0(r, t=0) = 5.0 \times 10^{23} \text{ m}^{-3}$, $N_i(r, t=0) = 0 \text{ m}^{-3}$ ($i = 1, 2, 3$). Thus, the atomic population densities obey the following rate equations:

$$\begin{aligned} \frac{\partial N_3(r, t)}{\partial t} &= P_g(t)N_0(r, t) - \frac{N_3(r, t)}{\tau_{32}}, \\ \frac{\partial N_2(r, t)}{\partial t} &= \frac{N_3(r, t)}{\tau_{32}} + \frac{1}{\hbar\omega_a} \mathbf{E}(r, t) \cdot \frac{\partial \mathbf{P}(r, t)}{\partial t} - \frac{N_2(r, t)}{\tau_{12}}, \\ \frac{\partial N_1(r, t)}{\partial t} &= \frac{N_2(r, t)}{\tau_{12}} - \frac{1}{\hbar\omega_a} \mathbf{E}(r, t) \cdot \frac{\partial \mathbf{P}(r, t)}{\partial t} - \frac{N_1(r, t)}{\tau_{10}}, \\ \frac{\partial N_0(r, t)}{\partial t} &= \frac{N_1(r, t)}{\tau_{10}} - P_g(t)N_0(r, t), \end{aligned}$$

where Gaussian pump $P_g(t) = P_0 e^{-(t-t_p/\tau_p)^2}$, with $P_0 = 3 \times 10^9 \text{ s}^{-1}$, $t_p = 6 \text{ ps}$ [18], and $\tau_p = 0.15 \text{ ps}$.

In order to solve the response of the active materials in the electromagnetic fields numerically, the finite-difference time-domain technique is utilized [19], using an approach similar to the one outlined in Ref. [20].

The object of our studies is to present pump-probe simulations on arrays of silver split-ring resonators (SRRs)

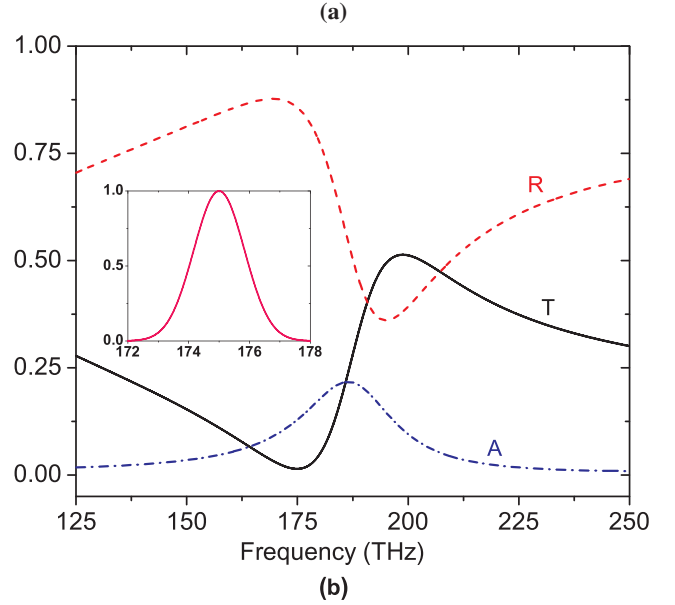
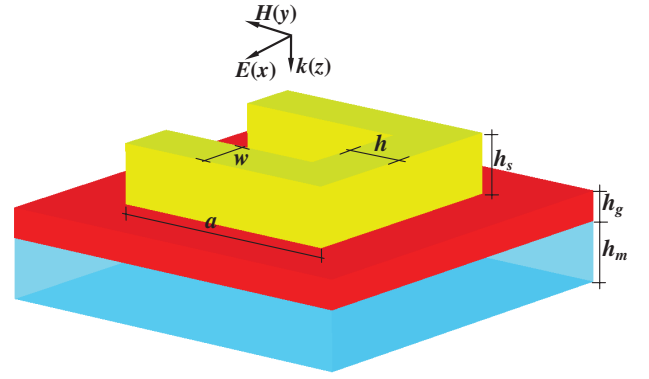


FIG. 2 (color online). (a) Schematic of the unit cell for the silver-based SRR structure (yellow) with the electric field polarization parallel to the gap. The dielectric constants ϵ for gain (red) and GaAs (light blue) are 9.0 and 11.0, respectively. (b) Calculated spectra for transmittance T (black), reflectance R (red), and absorbance A (blue) for the structure shown in Fig. 2(a). The inset shows the profile of the probe pulse with a center frequency of 175 THz (FWHM = 2 THz).

coupled to single quantum wells [11,12]. The structure considered is a U -shaped SRR fabricated on a gain-GaAs substrate with a square periodicity of $p = 250 \text{ nm}$ [see Fig. 2(a)]. The SRR is made of silver with its permittivity modeled by a Drude response: $\epsilon(\omega) = 1 - \omega_p^2/(\omega^2 + i\omega\gamma)$, with $\omega_p = 1.37 \times 10^{16} \text{ rad/s}$ and $\gamma = 2.73 \times 10^{13} \text{ rad/s}$. The incident wave propagates perpendicular to the SRR plane and has the electric field polarization parallel to the gap [see Fig. 2(a)]. The corresponding geometrical parameters are $a = 150 \text{ nm}$, $h_d = 40 \text{ nm}$, $h_g = 20 \text{ nm}$, $h_s = 30 \text{ nm}$, $w = 50 \text{ nm}$, and $h = 75 \text{ nm}$. Figure 2(b) shows the calculated spectrum (without pump) of transmittance T , reflectance R , and absorbance A for the structure shown in Fig. 2(a). The resonant frequency is around 175 THz, and

we refer to the resonant frequency according to the dip of the transmittance. In our analysis, we first pump the active structure [see Fig. 2(a)] with a short intensive Gaussian pump pulse $P_g(t)$ [see Fig. 3, top panel]. After a suitable time delay (i.e., the pump-probe delay), we probe the structure with a weak Gaussian probe pulse with a center frequency close to the SRR resonance frequency of 175 THz. Typical examples for the spatial distribution of electric field and gain are shown in Ref. [21]. The incident electric field amplitude of the probe pulse is 10 V/m, which is well inside the linear response regime. Then, we can Fourier transform the time-dependent transmitted electric field and divide by the Fourier transform of the incident probe pulse to obtain the spectral transmittance of the system as seen by the probe pulse. Additionally, we obtain the total pulse transmittance by dividing the energy in the transmitted pulse by the energy in the incident pulse, integrated in the time domain. We define the differential transmittance $\Delta T/T$ by taking the difference of the measured total plus transmittance with pumping the active structure minus the same without pumping and dividing it by the total plus transmittance without pumping. This differential transmittance is a function of the pump-probe delay. The bottom panel in Fig. 3 gives a differential transmittance $\Delta T/T$

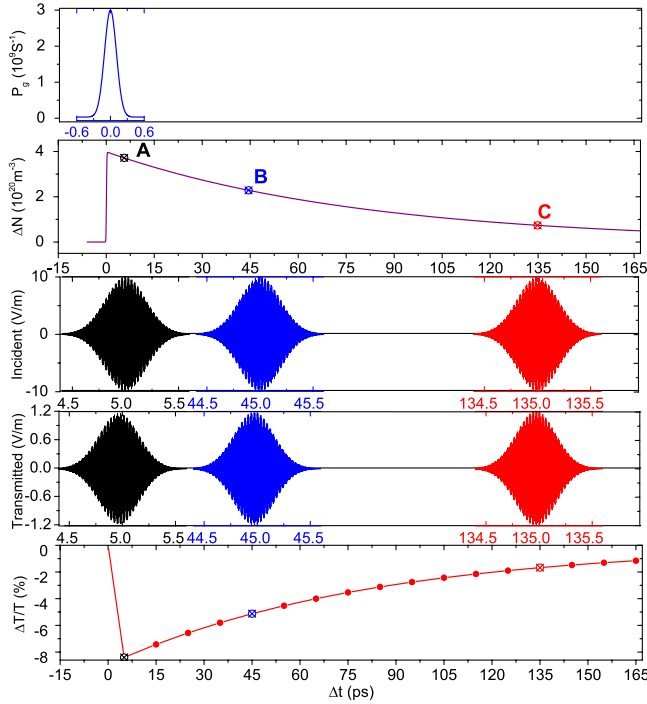


FIG. 3 (color online). Schematic of the numerical pump-probe experiments for the case on resonance. From the top to the bottom, each row corresponds to the pump pulse, population inversion, incident signal (with time delays 5, 45, and 135 ps), transmitted signal, and differential transmittance $\Delta T/T$. It should be mentioned here that the incident frequency of the probe pulse is 175 THz with a FWHM of 2 THz and is equal to the SRR resonance frequency.

which is negative. This result was not expected, and we need to understand this behavior, which agrees with the experiments [11,12].

Figure 4 gives an overview of the results obtained for the case of the SRRs on resonance, i.e., $\omega_a = 2\pi \times 175 \times 10^{12}$ rad/s. Data for the structure in Fig. 2(a) (left column in Fig. 4) and for the bare gain case (right column in Fig. 4) without the SRRs on top is shown. For parallel polarization, the light does couple to the fundamental SRR resonance; for perpendicular polarization, it does not. The probe center frequency decreases from top (179 THz) to bottom (169 THz). Note that the width of the probe spectrum is 2 THz [see the inset in Fig. 2(a)]. Hence, the data have been taken with 2-THz spectral separation. Inspection of the left column shows a rather different behavior for the SRRs with gain compared to the bare gain case. While the bare gain always delivers positive $\Delta T/T$ signals below +0.16% (right column) over the whole probe spectrum, the sign and magnitude of the signals change for the case SRRs with gain. Under some conditions, $\Delta T/T$ reaches values as negative as -8.50% around $f_{\text{probe}} = 175$ THz. Additionally, we may also get positive $\Delta T/T$ at the very edges of the probe range (see the left column in Fig. 4). If we turn to the case of perpendicular polarization, no distinct change between the pump-probe results on the SRRs (not shown in Fig. 4) and the bare gain (right column in Fig. 4), neither in the magnitude nor in the dynamics of the $\Delta T/T$, can be detected.

We argue that the distinct behavior can be attributed to the strong coupling between the resonances of the SRRs and the gain medium. The negative $\Delta T/T$ are not as we expected at first glance: The pump lifts electrons from the ground state to an excited state so that the absorption of the probe pulse is reduced, leading to an increase of

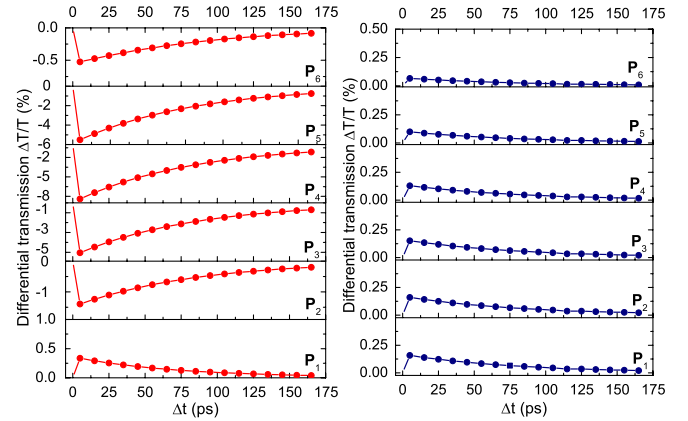


FIG. 4 (color online). Time domain numerical pump-probe experiments results for the SRR that is nearly on-resonant with the gain material. The left column corresponds to the parallel probe polarization with respect to the gap of the SRRs; the right column is the case for bare gain material, i.e., without SRRs on the top of the substrate. The width of the probe signal is 2 THz with decreasing in the probe center frequency from 179 THz for the top panel to 169 THz for the bottom panel.

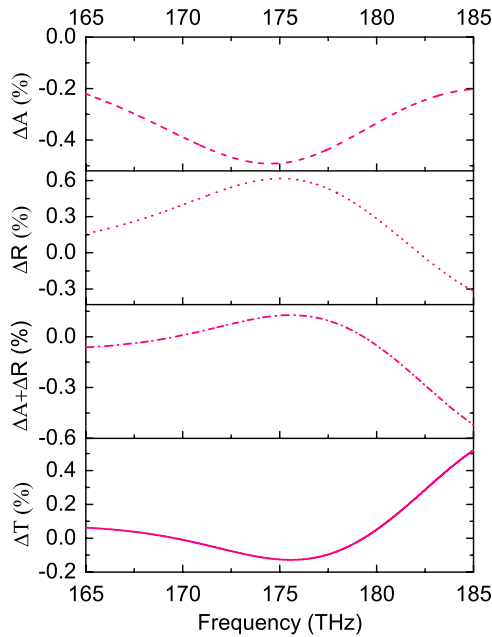


FIG. 5 (color online). Frequency domain numerical pump-probe experiments results for the on-resonance case. Simulations results for the differences in transmittance (ΔT), reflectance (ΔR), and absorbance (ΔA) versus frequency.

transmission. This is not the whole story. The reason lies in the fact that with the pump we not only affect the absorption but disturb the reflection of the structure, resulting in the mismatching of the impedance. Furthermore, we observed either an increasing or a decreasing tendency for the case of on resonance as shown in Fig. 4. All those behaviors can be explained by the competing of the weak gain resonance and the impedance mismatching between pump and without pump cases. We will explore the underlying mechanism below. Figure 5 shows the results for the difference in absorbance (ΔA), difference in reflectance (ΔR), their sum ($\Delta A + \Delta R$), and the difference in transmittance [$\Delta T = -(\Delta A + \Delta R)$] between pump ($P_0 = 3 \times 10^9 \text{ s}^{-1}$) and no pump using a wide probe (FWHM = 54 THz) pulse with a fixed pump-probe delay of 5 ps. As expected, we may observe a positive differential transmittance, $\Delta T/T > 0$, when we pump the gain, $\Delta A < 0$, and if ΔR (impedance match) remains unchanged.

The results of Fig. 5 are obtained for pump-probe experiments with the probe frequency equal to the resonance frequency of the SRRs (175 THz) at a pump-probe delay of 5 ps; results for longer pump-probe delays are shown in Supplemental Material [21]. Notice that ΔR is positive, ΔA is negative, and ΔT is also negative very close to the resonance frequency. If the probe center frequency moves away from the SRR resonance frequency, the negative $\Delta T/T$ decreases in magnitude, and finally $\Delta T/T$ becomes positive. These results are shown in Fig. 6 and agree with experiments [11,12]. If we can increase the magnitude of the Gaussian pump pulse $P_g(t)$ to $5 \times 10^{10} \text{ s}^{-1}$ and we repeat the pump-probe experiments, $\Delta T/T \approx -100\%$ at

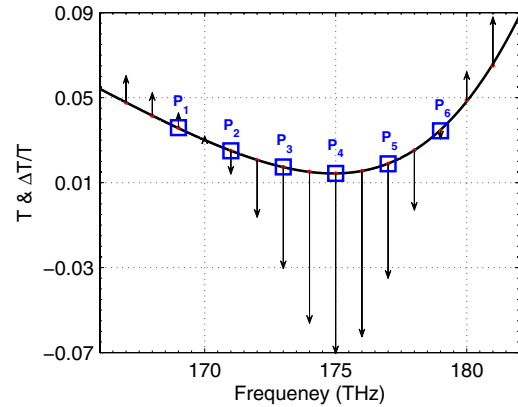


FIG. 6 (color online). The transmittance T (without pump, solid line) and the on-resonance differential transmittance $\Delta T/T$ results (vector arrow). The direction and the length of the arrow stand for the sign and the amplitude of $\Delta T/T$, respectively. The squares from P_1 to P_6 correspond to the frequency of probe pulse ranging from 169 to 179 THz with uniform step of 2 THz.

resonance frequency, 175 THz. If we increase the pump amplitude further to 10^{11} s^{-1} , we can compensate for the losses. However, such pump intensities are unrealistic experimentally [21]. In conclusion, we have introduced a new approach for pump-probe simulations of metallic metamaterials coupled to gain materials. We study the coupling between the U -shaped SRRs and the gain material described by a four-level gain model. Using pump-probe simulations, we find a distinct behavior for the differential transmittance $\Delta T/T$ of the probe pulse with and without SRRs in both magnitude and sign (negative, unexpected, and/or positive). Our new approach has verified that the coupling between the metamaterial resonance and the gain medium is dominated by near-field interactions. Our model can be used to design new pump-probe experiments to compensate for the losses of metamaterials.

Work at Ames Laboratory was supported by the U.S. Department of Energy (Basic Energy Science, Division of Materials Sciences and Engineering) under Contract No. DE-ACD2-07CH11358. This work was partially supported by the European Community FET project PHOME (No. 213390) and by Laboratory-Directed Research and Development Program at Sandia National Laboratories. Z. H. gratefully acknowledges the support of the National Natural Science Foundation of China (No. 60931002 and No. 61101064), Distinguished Natural Science Foundation (No. 1108085J01), and Universities Natural Science Foundation of Anhui Province (No. KJ2011A002).

-
- [1] V. M. Shalaev, *Nature Photon.* **1**, 41 (2007).
 - [2] C. M. Soukoulis, S. Linden, and M. Wegener, *Science* **315**, 47 (2007).
 - [3] C. M. Soukoulis and M. Wegener, *Science* **330**, 1633 (2010); *Nature Photon.* **5**, 523 (2011).

- [4] A. Fang, Th. Koschny, and C. M. Soukoulis, *Phys. Rev. B* **82**, 121102(R) (2010).
- [5] S. Wuestner, A. Pusch, K.L. Tsakmakidis, J.M. Hamm, and O. Hess, *Phys. Rev. Lett.* **105**, 127401 (2010); *Phil. Trans. R. Soc. A* **369**, 3525 (2011).
- [6] A. Fang, Z. Huang, Th. Koschny, and C. M. Soukoulis, *Opt. Express* **19**, 12 688 (2011).
- [7] Y. Sivan, S. Xiao, U.K. Chettiar, A.V. Kildishev, and V.M. Shalaev, *Opt. Express* **17**, 24 060 (2009).
- [8] S. Xiao, V.P. Drachev, A.V. Kildishev, X. Ni, U.K. Chettiar, H.-K. Yuan, and V.M. Shalaev, *Nature (London)* **466**, 735 (2010).
- [9] E. Plum, V.A. Fedotov, P. Kuo, D.P. Tsai, and N.I. Zheludev, *Opt. Express* **17**, 8548 (2009).
- [10] K. Tanaka, E. Plum, J.Y. Ou, T. Uchino, and N.I. Zheludev, *Phys. Rev. Lett.* **105**, 227403 (2010).
- [11] N. Meinzer, M. Ruther, S. Linden, C.M. Soukoulis, G. Khitrova, J. Hendrickson, J.D. Olitzky, H.M. Gibbs, and M. Wegener, *Opt. Express* **18**, 24 140 (2010).
- [12] N. Meinzer, M. König, M. Ruther, S. Linden, G. Khitrova, H.M. Gibbs, K. Busch, and M. Wegener, *Appl. Phys. Lett.* **99**, 111104 (2011).
- [13] D.J. Bergman and M.I. Stockman, *Phys. Rev. Lett.* **90**, 027402 (2003).
- [14] M.I. Stockman, *Nature Photon.* **2**, 327 (2008).
- [15] R.F. Oulton, V.J. Sorger, T. Zentgraf, R.-M. Ma, C. Gladden, L. Dai, G. Bartal, and X. Zhang, *Nature (London)* **461**, 629 (2009).
- [16] M. A. Noginov, G. Zhu, A. M. Belgrave, R. Bakker, V. M. Shalaev, E. E. Narimanov, S. Stout, E. Herz, T. Suteewong, and U. Wiesner, *Nature (London)* **460**, 1110 (2009).
- [17] A. E. Siegman, *Lasers* (University Science, Sausalito, CA, 1986), Chaps. 2, 3, 6, and 13.
- [18] The pumping rate is equivalent to a pump intensity. The pump power density is equal to $\hbar\omega_a P_g N_0$, and the pump intensity $I_p = (\text{pump power})/(\text{surface area}) = \hbar\omega_a P_g N_0 (\text{volume})/(\text{surface area}) = \hbar\omega_a P_g N_0 d$, and d is the thickness of the gain layer. If we use the numbers of our simulations, $P_g = 3 \times 10^9 \text{ s}^{-1}$, $N_0 = 5 \times 10^{23} \text{ m}^{-3}$, $\omega_a = 2\pi \times 175 \text{ THz}$, and $d = 20 \text{ nm}$, then $I_p = 3.5 \text{ W/mm}^2$.
- [19] A. Taflove, *Computational Electrodynamics: The Finite Difference Time Domain Method* (Artech House, London, 1995), Chaps. 3, 6, and 7.
- [20] A. Fang, Th. Koschny, and C. M. Soukoulis, *J. Opt.* **12**, 024013 (2010).
- [21] See Supplemental Material at <http://link.aps.org/supplemental/10.1103/PhysRevLett.108.187402> for additional details of the simulations and a discussion of over-compensation of the loss.